Zinc and cobalt nano ferrites and their potential applications in environmental sustainability

Leena V. Hublikar
KLE Technological University
Sharanabasava V Ganachari (sharanu14@gmail.com)
KLE Technological University https://orcid.org/0000-0002-9895-1829
Jayachandra S. Yaradoddi
KLE Technological University
Aasim U. Mokashi
KLE Technological University

Research Article

Keywords: Nano ferrites, co-precipitation method, Fourier-transform spectroscopy (FTIR), X-ray powder diffraction (XRD), Field Emission Scanning Electron Microscope (FESEM), chemical vapor sensing study, water analysis, absorption and Adsorption studies

Posted Date: March 25th, 2020

DOI: https://doi.org/10.21203/rs.3.rs-18423/v1

Zinc and cobalt nano ferrites and their potential applications in environmental sustainability

Leena V. Hublikar [b, c], Sharanabasava V. Ganachari* [a,b], Jayachandra S. Yaradoddi [a], Aasim U. Mokashi

[a] Centre for Material Science, School of Mechanical Engineering, KLE Technological University, BVB campus, Vidyanagar Hubbalii-580031, Karnataka, INDIA

[b] Department of Chemistry, KLE Technological University, BVB campus, Vidyanagar Hubbalii-580031, Karnataka, INDIA

[c] Department of Chemistry, KLE's P. C. Jabin Science College, Vidyanagar, Hubballi-580031, Karnataka, India

Abstract:

Fundamental research and industrially applied research, currently depend on magnetic oxide nanoparticles and ferromagnetic oxides due to their extensive applications for electronic, magnetic, optical sensor and absorptive activities. ferromagnetic substances mainly contain a different type of Ferrite. Ferrite material constitutes, Iron oxide (Fe_2O_3) and divalent metal oxides of Transition metals like cobalt, nickel etc. The key objective of this paper is to study the impending applications of nano - ferrites doped with bivalent transition metals with their properties. Low-Temperature Self-Propagating combustion method was used to synthesize the particles. Synthesized Zinc and Cobalt Nano ferrites from the chemical co-precipitation method were found to be of 20 to 90 nm in average size, and comparative study of their properties using the results of Fourier-transform spectroscopy (FTIR) and X-ray powder diffraction (XRD). The Field Emission Scanning Electron Microscope (FESEM) confirms the conception of ferrite nanoparticles with a structure type cubic spinel. Further comparative Sensing studies showed that the sample displays variation in resistance when gases are passed over the surface, and the change in resistance is observed.

Keywords: Nano ferrites, co-precipitation method, Fourier-transform spectroscopy (FTIR), X-ray powder diffraction (XRD), Field Emission Scanning Electron Microscope (FESEM), chemical vapor sensing study, water analysis, absorption and Adsorption studies.

***corresponding author**

INTRODUCTION

In an era where compactness of various devices is of prime importance, nanomaterials can play a central role[1]. Science is built on a large number of very small nanoparticles. Which are acting as powerhouses of materials[2]. Materials gain a verity of Chemical & physical properties depending on the size and shapes of these nanoparticles[1,3]. Properties, such as electrical and optical, display unique significant differences from the bulk properties[1].

The small material properties change considerably when they are brought to nano magnitude, of the order of 100 nm or less[4]. Being a particular type of such nanoparticles, the ceramic nanomaterials, had a wide variety of applications[4,5]. They are known for their stability, availability of information on relatively cheaper synthesis techniques[6,7]. Typically, $MeFe_2O_4$ is common formula for spinel ferrite (SF). Where Me indicates one or different types of a bivalent transition metal like Mn, Zn, Co, Ni, Cu, etc.[8] [9] ferrite fabrication procedures, Traditionally involve the grinding and calcination of binary metal oxide mixtures repeatedly to obtain pure ferrite phase [10]. These methods often follow the solid-state transformation, which involves high-temperature annealing, ball milling, and other complex sintering protocols leading to the anticipated microstructure and engineered shapes[5]. This also improves homogeneity and particle size distribution, other significant properties of the final product[11].

Many works are going on metal ions substitution in nano- ferrites. Researchers, getting Interested nowadays in ferrites Substituted with rare-earth ions[12–16], which have changed the physical as well as chemical (magnetic and electrical) properties of nanoparticles[17] and that intern depends upon nature and ionic radii of element substituted and its particle size[4]. Further applications in magnetism is tailored by decreasing particle size, altering the cation distributions with different ions at the lattice (tetrahedral and octahedral) sites[18]. Specific applications of nano ferrites require prominent properties in nanomaterials[10]. In the case of Ceramics, parameters of Nanostructured ferrites initially decrease to some extent with grinding,

and with further milling, it increases[19]. A decrease in the grain size increases magnetization and also found that cation inversion is attributed to change in the lattice and its values [19,20].

Amongst the category of SF's, $CoFe_2O_4$ and $ZnFe_2O_4$ have expanded more attention of researchers owing to numerous valuable properties. More chemical stability, extraordinary mechanical hardness, and good coercivity[21]. The properties of $CoFe_2O_4$ and $ZnFe_2O_4$ can be enhanced by adding metal ions with different valency, coordinating to requirements[22]. The substitution of rare-earth ions in cobalt and Zinc ferrites made the study more interesting[23]. This is due to their vast applications in many devices such as electromagnetic wave absorbers, inductor cores, converters and many more[24]. By following disciplined fabrication processes, divalent Co^{2+} resides at tetrahedral lattice and trivalent Fe^{3+} ions at octahedral sites can be tailored.[25],[26] and we also emphasized from the previous research that, part of Co^{2+} ions present at the octahedral sites are responsible for the physical properties of $CoFe_2O_4$.That is the preference of accumulation of Co^{2+} ions will be influencing the magnetic property, improving the resistive properties and reduces dielectric loss[25,27].

By combining different types of reactions, extremely controlled shapes (spherical or cubic) can be achieved. Fine quality spinel cobalt ferrite ($CoFe_2O_4$) and monodisperse nanocrystals can be synthesized[28]. Owing to controlling nanocrystal, growth shape, can be can also be oscillated between spherical and cubic. Not only this, but also blocking temperature and magnetization of nanoparticles resolute by the size, irrespective of their structure. The nanoparticles structure is a leading factor aimed at the coercivity Factor for nanocrystals due to their superficial anisotropy[29]. And these magnetic nanoparticles due to their high capacity to store information got tremendous technological applications [25,30] The typical spinel structure represented as $(M_{1-x}Fe_x)$ $[M_xFe_{2-x}]O_4$ (M is the metal ion) has a 32 O^{2-} anions, in between these at a particular interstitial sites metal ion are distributed and ideally termed as the face-centered cubic unit cell[31]. In that coordination compounds, round brackets indicate

tetrahedral (X site) and square brackets designate the and octahedral (Y site), and x implies the inversion parameter[32]. Based on the composition of divalent metal ions in tetrahedral and octahedral sites, spinel structures are categorized as normal, inverse and partially inverse. Quantity of these divalent metal ions decided by the synthesis, annealing processes and also on particle size[29]. $CoFe_2O_4$ and $ZnFe_2O_4$ are spinels, but the arrangement of the ions among the lattice sites I unique.

Another burning issue for social awareness is to control water pollution[33,34]. Our environment is commonly distributed with Heavy metals around[31]. All types of ecological pyramids are affected by these. many industrial effluents and everyday human activities due to the increased technology are the causes[30]. With the knowledge of the literature survey in wastewater treatment attempted to control the toxicity by adsorbing with cobalt and zinc nano ferrites synthesized in our laboratory.

Bivalent transition metals like cobalt and zinc are with doped with nano - ferrites they're by following Low-Temperature Self-Propagating combustion method[8,16,35,36]. Synthesized Zinc and Cobalt Nano ferrites from the chemical co-precipitation method were confirmed with standard data of literature, found to be of 20 to 90 nm in average size, and comparative study of their properties using the results of FTIR and XRD. The SEM confirms the cubic spinel structure formation of ferrite particles. Absorption[37] and adsorption [38,39]studies are done with laboratory wastewater and conventional laboratory dyes. Comparative Sensing studies showed that the sample displays variation in resistance when gases are passed over the surface and the change in resistance is observed.

MATERIALS AND METHODS

The present context is to design the synthesis Cobalt and Zinc ferrite and compare its properties by different characterization methods.

Low-Temperature Self-Propagating combustion method was used to synthesize the nanoparticles[40–42]. Simple precursors employed were Ammonium Iron (II) Sulfate ((NH4)2Fe(SO4)2·6H2O SDFine-Chem ltd., AR grade), oxalic acid (AR grade)and respective salts of $ZnCl_2$,$CoCl_2$(SDFine-Chem ltd., AR grade), which were weighed for the desired stoichiometric ratio and dissolved in double-distilled water[43]. The mixture, using a magnetic stirrer was stirred for 1 h, a precipitate of constant metal oxalate was obtained at room temperature. The precipitate was heated with the fuel polyvinyl alcohol ($[CH_2CH(OH)]_n$) in hot air oven to obtain a colored powdered sample of the nano- ferrites of Zinc and cobalt.

CHARACTERIZATIONS

To analyze the structure of nanoparticles, XRD Diffractometer (Xpert MPD, Make: Philips, Holland) was employed. The XRD patterns were recorded on the X-ray diffractometer at the range of 2θ from 3º to 136º, using Cu target X-Ray tube, Cu Kα (λ = 1.5406 A) radiation with an accelerating voltage of 40 kV. FT-IR study was accomplished in order to confirm the formation of nano particle in the range of 4500-400 cm-1by instrumentation, Using NICOLET 6700, USA instruments. To analyze morphological features of nanoparticles, field emission scanning electron microscope was used at an accelerating voltage With LaB6 filament -2nm 30 KV With W filament 3.5nm at 30 kv by Emission current of 0 to 200 μA and accelerating Voltage: 0.2 to 30 kv.

RESULTS AND DISCUSSION:

1. X-ray diffraction analysis (XRD):

The XRD peaks, structural analysis of $CoFe_2O_4$ and $ZnFe_2O_4$ nanosamples, were studied with Sherrer's equation, the average particle size obtained varied between 18.54-18.90 nm based on the 2θ value which was found to be 35.64,40.58.70 and 62.60 respectively. sample

possessed a cubic spinel structure[44]. Size and shapes define the XRD peak position and intensity defines the atomic position of the unit cell.

The micro strains by definition, root mean square of the variations in the lattice parameters across the sample is calculated and were found to be 66.14, 71.27, and 81.54, for cobalt ferrites. This implies the decrease of the lattice parameters when the more prominent ion is partially substituted by the smaller one. The XRD patterns are perfectly matched with the standard XRD pattern with reference code ICSD 00-001-1121, indicating purity of the synthesized material.

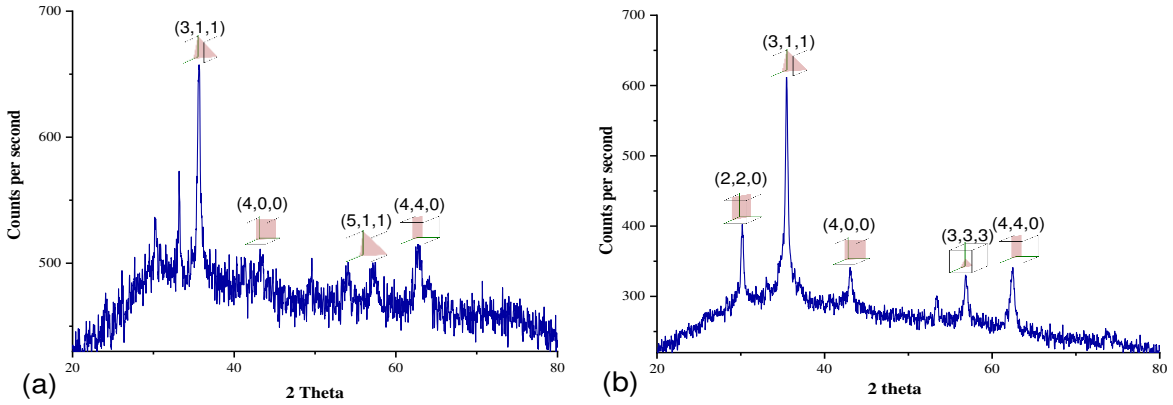

Figure 1 (a) & 1 (b): XRD peaks of spinel nano ferrites

Similarly, for zinc ferrite, the average particle size obtained varied between 18.63-20.45 nm based on the 2θ value, which was found to be 30.30, 35.45,43.05, and 56.85, respectively[40]. The micro strains were calculated and were found to be 48.28, 77.86, and 37.39. Cubic phase structure of the zinc ferrite rendered by the JCPDS 22-1012 card.

Nano Cobalt ferrite				
2θ	ƛ	particle size (nm)	dislocation density	micro strain
27.6962	545	18.54	0.539	66.14
33.2055	595	18.78	0.532	71.27
35.539	685	18.9	0.53	81.54
Nano zinc ferrite				

2θ	ƛ	particle size	dislocation density	micro strain
30.1008	400	18.63	0.536	48.28
35.4579	654	18.89	0.529	77.86
56.7441	340	20.45	0.49	37.39

Table. 1.XRD values of metal nano ferrite

2. Fourier-Transform -Infrared Spectroscopy (FTIR)

An important tool, Infrared spectroscopy which made an investigation of the spinel structural formation of ferrite nanoparticles. This provides information about positions of the metal cation in the spinel structure and their vibrational modes. In the case of ferrites, the oxygen ions vibrate with cations of the unit cell in the octahedral and tetrahedral sites are responsible for absorptions bands. For spinel ferrites, a specific region of absorption is in the range of 400–600 cm. Cobalt nano-ferrite exhibits two absorption bands in this region. High vibration band at 557.22cm and others were at 446.6cm. Absorption bands detected within this edge disclose the creation single-phase spinel structure having two sub-lattices, octahedral and tetrahedral. $CoFe_2O_4$ is exhibiting an inverse spinel where Fe^{3+} ions and Co^{2+} ions present at the tetrahedral and octahedral lattice sites respectively[38]. The vibration observed due to bending was very broad. The reason could be attributed to the distribution of Fe^{3+} ions leading to vibrations due to the stretching mode of the (Fe^{3+})–oxygen bond at tetrahedral, and other caused due to $(Co^{2+})^-$ oxygen vibrations in octahedral sites.

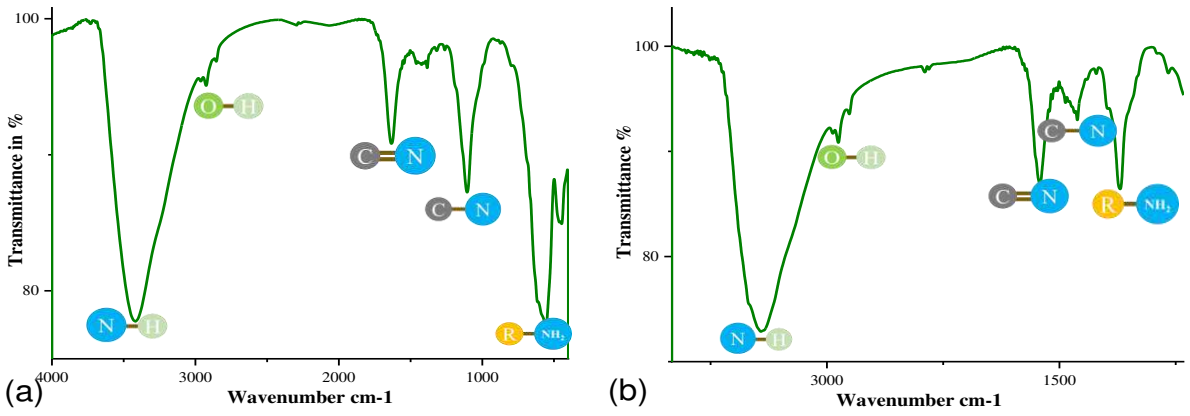

Figure. 2 (a) & 2 (b): FTIR bands of spinal nano ferrites

3.Scanning electron microscopy (SEM):

Images of SEM reveal surface topography and composition of the sample. The surface morphological images and Microscopic structure shows a good agreement with XRD results of ferrite nanoparticles. Images suggest that morphology at the surface is porous in nature, it is happening because of the significant degree of agglomeration of ferrite particles.

SEM Image Nano Cobalt ferrites show a zoomed view of the powdered sample, illustrated with both large and small grains. The nanoparticles size was found to be 50 nm. The surface is wavy, with an average surface roughness value of about 12.34 nm. From the images shown above, we can infer that the particles are of irregular shape and are agglomerated together to form a bigger particle. There was a considerable trace of carbon seen[45]. The agglomeration of the particles may be due to the hydrophilic nature of the extract added. The traces of carbon observed may be due to the usage of the mica sheet as a substrate for the sample.

(a) SEM image and surface texture patterns of Cobalt nanoferrites	(b) SEM image and surface texture patterns of Zinc nanoferrites
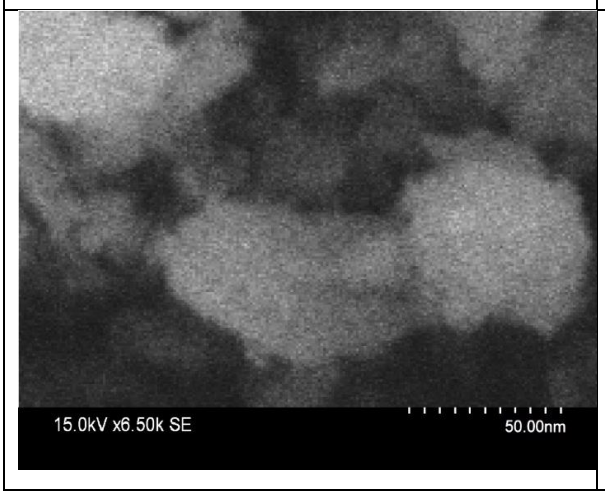	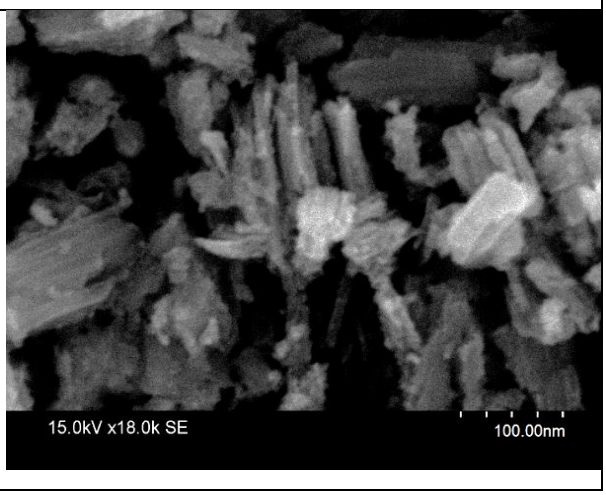

Figure. 3 (a) & 3(b). SEM images of spinal nano ferrites

SEM Image Nano Zinc ferrites show the size of the particle is around 90 nm. The average roughness value is 7.35 nm. From the images shown above, we can infer that the

particles are of irregular shape and agglomerated together. There was a significant trace of carbon seen. The agglomeration of the particles may be due to the hydrophilic nature of the extract added. The traces of carbon observed may be due to the usage of the mica sheet as a substrate for the sample.

APPLICATIONS STUDIES

1. Gas sensing mechanism:

Spinal ferrites operate in the same gas sensing mechanism as that of semiconductors. In spinal ferrites, oxygen chemisorption leading to divalent metal ions also to oxidized in their octahedral sites. Then a change in electrical conductivity occurs due to trapping of electrons. When gas molecules come in contact with these oxygens, they take back the electrons and shows the sensing activity.

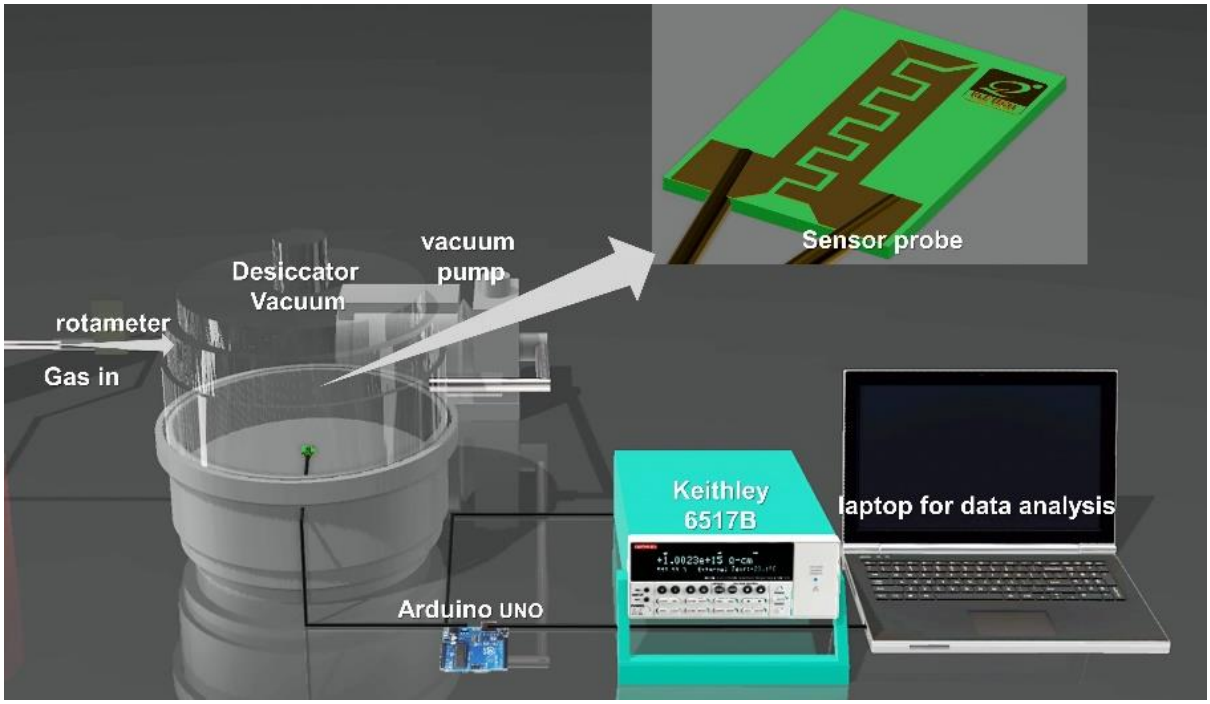

Figure. 4 chemical vapor sensing arrangement

By generating a vacuum in a closed chamber (shown in above figure 4), a setup was made where the probe which was coated with the sample was placed. Gases from various chemicals were made to pass through the chamber with the help of a nozzle from another container. An Arduino UNO was used which was connected to the probe to detect the change in voltages. A program to detect these changes was uploaded to the Arduino UNO. Now, as the probe senses the gas, there is a variation in the voltage, which indicates that gas has been sensed. This variable voltage gives rise to a variable resistance. [19] The sensing was taken at room temperature. The gases that were used are acetone, ethyl alcohol, methanol, and ammonia. Using a Keithley meter, the value of change in resistance (shown in figure 5) was found which can also be calculated using the formula,

$$R_s = \frac{V_S - V_r}{V_r} R_r$$

Where R_s = required a change in resistance

R_r = resistance across reference

V_s = supply voltage

V_r = drop in voltage

Thus, for cobalt nano ferrite, resistance values of these gases are in order methanol > acetone > ethanol > ammonia. Then sensitivity of these gases is in reverse order that is methanol < acetone < ethanol < ammonia for cobalt nano ferrite.

(a) Nano cobalt ferrite **(b) zinc nano ferrites**

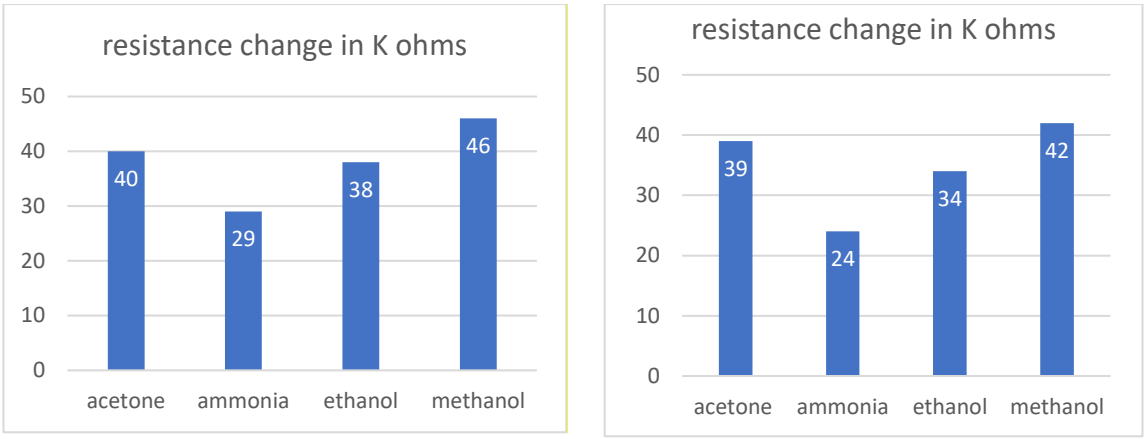

Figure 5: (a) & (b) Bar graph of relative sensing properties with different gases

Thus, for zinc nano ferrite, resistance values of these gases are in order, methanol> acetone > ethanol > ammonia. Then sensitivity of these gases is in reverse order that is methanol < acetone < ethanol < ammonia.

2. Wastewater analysis:

SEM results show the porous nature of nano ferrites synthesized. In accordance with this wastewater analysis and adsorption studies are made. Sample X, is wastewater it is collected by the chemistry laboratory of P C Jabin science college Hubballi. Then 10 mg Cobalt nano ferrites (B2) and Zinc nano ferrites (B4) are added to 20ml of Waste sample shaken well and given for water analysis at ESSAR laboratories and Research Centre at approved by AGEMARK grading Keshwapur Hubballi.

Parameters	**Sample-X**	**Sample – B2 (Co-nanoferrite)**	**Sample – B4 (Zn-nanoferrite)**
Turbidity (NTU)	250	220	180
Hydrogen ion concentration (pH)	11.5	11.4	10.4
Electric conductivity (µS)	3140	4600	2280
Total dissolved solids-TDS (Mg/L)	1880	2760	1370
Chloride (Mg/L)	467	666	368
Fluoride (Mg/L)	0.8	0.6	0.5
Sulphates (Mg/L)	40	56	36
Nitrates (Mg/L)	10	15	10

Iron (Mg/L)	0.6	0.6	0.6
Alkalinity (Mg/L)	1100	1600	700
COD(Mg/L)	60.4	68.8	52.4
BOD(Mg/L)	7.4	8.4	5.6

Table.2. Water analysis reports with nanoferrites

Turbidity: Turbidity indicates the number of suspended sediment solids in water. Higher is the turbidity, and more are the suspended sediments in it. Reports show that turbidity values decrease from waste sample to B4 sample. This nature of synthesized nano ferrites metal absorption, from sample X. Absorption capacity, is more in sample B4.

Hydrogen ion concentration (pH): As in report pH value decreases from the waste sample, shows acidity of water decreases. The decrease is sharply noted at B4sample. The concentration of hydrogen ions in water determines the pH value. Alkalinity is the capacity of water to neutralize acids. That is it is the measure of the struggle of water to the lowering of pH when acids are added to the water [46].

Electrical conductivity (EC): EC, of the water, specifies the purity of water. And the number of total dissolved salts (TDS) in water measures the conductivity of water. It is a measure of the capability of water to carriage the electricity. It increases as salinity increases. Fewer ions in the water, less is the EC, purer is the water sample. B4 sample adsorbed the number of ions, appears to be pure.

Electrical conductivity increases with an increase of Chloride, sulphates and Nitrate content. Chloride, sulphate and nitrate content from wastewater are absorbed by the sample B4, remains with 368mg /l.0.5mg/li and 10mg/l, respectively. It shows that Zn nano ferrite can be used in waste treatment[46].

Chemical Oxygen Demand the measurement of total oxidizable chemicals in the water. It quantifies the amount of oxidizable pollutants found in wastewater.

The complete discussion reveals that synthesized nano ferrites shows the absorptive capacity. Which favors that these can be used in wastewater analysis.

3. Absorption:

The existence of a heavy concentration of constituent at the surface of a solid or liquid a phase is called Adsorption. The reason behind this is the existence of residual forces at the surface of the liquid or solid phase. The constituent on the surface of which adsorption occurs is denoted as Adsorbent. And Adsorbate is which is being adsorbed on substrate[47].

In this phenomenon, when a gas is adsorbed on a solid surface, ΔS is appears to be negative, as its movement is restricted leading to a decrease in the entropy. Now, this process is natural (spontaneous), that is ΔG is to be negative. But ΔS is becoming negative when adsorption takes place. Thus, according to the thermodynamic relationship of Gibbs free energy, $\Delta G=\Delta H-T\Delta S$ adsorption is always exothermic. Van der Waals forces (London Dispersion Forces), a type of weak forces of attraction is responsible for the Adsorption process[48]. The phenomena depend on both the nature of adsorbate and adsorbent along with pH, pressure, and surface area also.

In the case of adsorbents, the size of the pores at the surface and the functional groups are responsible for effective adsorption. Similarly, molecular states, solubility, and functional groups significantly express the nature of adsorbate.

In the current work, we deliberate the adsorption behavior of different concentrations of acetic acid, a weak acid on Synthesized nano ferrites. Different Isotherms are studied for this system and Langmuir model holds good for Zn nano ferrites. Langmuir isotherm explains the adsorption situation where the number of sorption sites available is limited. Because of which adsorption sites become saturated, to maximum capacity.

As acetic acid is a weak acid, it forms OH-groups when it reacts with water and which forms bonds with metal-nanoparticles at the surface. Such reactions act under particular pH of

the solutions, further OH group can be acting as a proton donor or acceptor of a proton, and balances the pH of the solution[49]. And according to the references, we found that more alcoholic groups present at adsorption interphase more is the adsorption. FTIR studies have given proof of this phenomenon.

Cobalt and Zinc nano ferrites hold good for the study of adsorption due to porosity. Absorption of acetic acid at room temperature is studied by absorption isotherm. Acetic acid of different concentrations is prepared by mixing the required amount of distilled water in glass wash bottles. Adsorbents cobalt and zinc nano ferrites are activated by heating them in ovens. When they become activated with open pores, weighed 1gm, and added to each bottle separately. Now all the four bottles were shaken well in electrical shakers for half an hour [50] and then kept in a water bath for separation for 2hours. After separation, 5ml of each sample is pipetted out carefully and titrated against the standard solution of sodium hydroxide.

Readings	**Sample B2 (Cobalt nanoferrite)**						**Sample B4(Zinc nanoferrite)**			
B.R(before A) ml	**Co (mg/L)**	**B.R (after A) ml**	**Ce(mg/L)**	**1/Ce**	**Qe(mg/g)**	**1/Qe**	**Ce(mg/L)**	**1/Ce**	**Qe(mg/g)**	**1/Qe**
23.3	0.499	21.9	0.468	2.1362	0.031	32.25	0.447	2.232	0.051	19.60
17.4	0.372	16.0	0.342	2.9154	0.030	33.33	0.325	3.086	0.049	20.36
11.4	0.244	10.2	0.218	4.0983	0.025	40.0	0.201	5.0	0.044	22.27
5.3	0.113	4.3	0.092	8.9285	0.020	50.0	0.079	12.82	0.034	29.41

Table 3 -Adsorption Details

Langmuir absorption isotherm:

The Langmuir isotherm is an actual isotherm for an explanation of monolayer formation on a surface containing a finite number of active adsorptive sites. And further, no more adsorption occurs.

Thus, Langmuir isotherm epitomizes metal ion, distribution between the liquid and solid phases[51]. For n-number of identical sites at the surface, Langmuir isotherm is valid up to monolayer adsorption.

Langmuir model assumes that vacant available sites are of equal size and shape on the surface of the adsorbent and uniform energies of adsorption. Based on assumptions, its equation is given as

$$R_L = \frac{1}{1+(1+K_L C_0)}$$ Ref [52]

C_0 = initial concentration

K_L= Langmuir Constant

R_L = separation factor

R^2 = equilibrium sorption

Zinc ferrite nanoparticle is showing optimum results for Langmuir isotherm, with equilibrium sorption value very much near to 1.and separation factor which shows the absorptive nature is advantageous that is greater than 0 and less than 1.

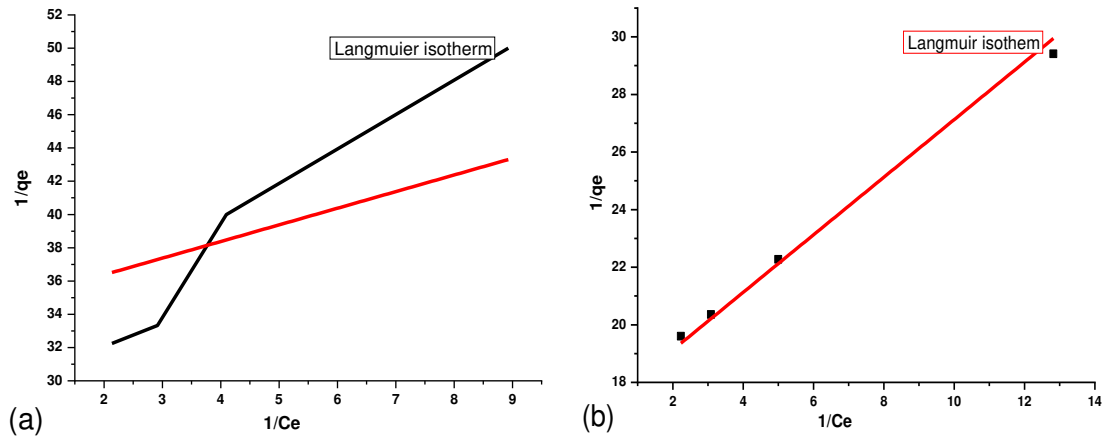

Figure 6 (a) & 4 (b): adsorption isotherms

4. Adsorption of Dyes:

The dye industry is one of the most water-consuming industries. Effluents of these industries contain many hazardous chemicals, including dyes. Proper advanced techniques are incorporated to remove these dyes and discharge into water bodies[53,54]. To do so synthesized

nano ferrites are examined with some laboratory dyes adsorption study, which may further minimize the risk of industrial effluents.

Different dyes and their Absorption spectrum are obtained by using the photo colorimeter of ELICO make. The optical density (O.D) readings of the dyes are obtained by taking water as standard, at their respective wavelengths, where color content an index of OD. Now different dyes are added with required (0.1mg) of cobalt ferrite nanoparticles. Then each test tubes are shaken well, and color change after adsorption are observed in figure 6. Similarly zinc ferrite nanoparticles are to be carried out. After dye adsorption studies, using the cobalt and zinc ferrite nanoparticles, and the O.D of the dyes was re-recorded at their respective nm, as in **table 4**, with different filters (wavelength). Color change is confirmed by optical density values, are tabulated in **table 5**.

Sl.No	**Dyes name**	**Chemical formula**	**Chemical structure**
1	Phenolphthalein	$C_{20}H_{14}O_4$	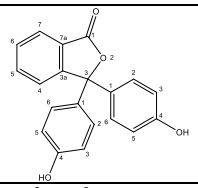
2	Aluminon	$C_{22}H_{23}N_3O_9$	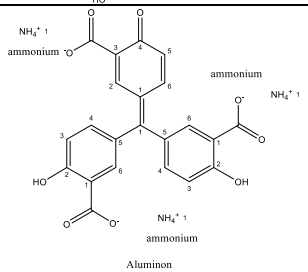 Aluminon
3	Methyl orange	$C_{15}H_{15}N_3O_2$	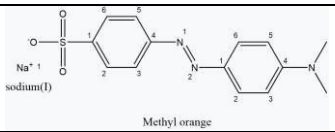 Methyl orange
4	Phenol red	$C_{19}H_{14}O_5S$	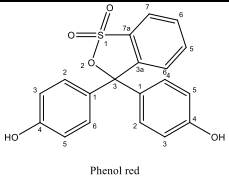 Phenol red
5	Methyl red	$C_{14}H_{14}N_3NaO_3S$	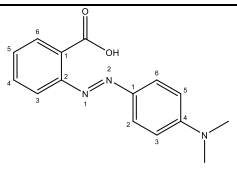 Methyl red

6	Methylene blue	$C_{16}H_{18}ClN_3S$	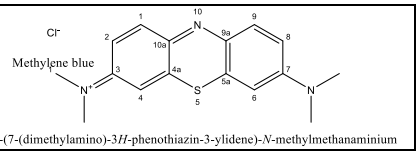

Table 4. Dyes and their Molecular formula

By using the formula given below the % dye adsorption was calculated

$$\% \text{ of dye adsorption} = \frac{\text{Initial O.D} - \text{final O.D} \times 100}{\text{Final O.D}}$$

Synthesized nanoparticles are showing active absorption active owing to the functional amino acid group, which is responded with dyes and removed from their aqueous solutions. It is evident that Cobalt ferrite NPs and Zinc ferrite NPs can be used as absorbents for different environmental dye pollutants. Further percentage of adsorption in comparison with cobalt and zinc shows that zinc nano ferrites are effective in dye adsorption for given dyes.

Dyes samples without nanoferrites			
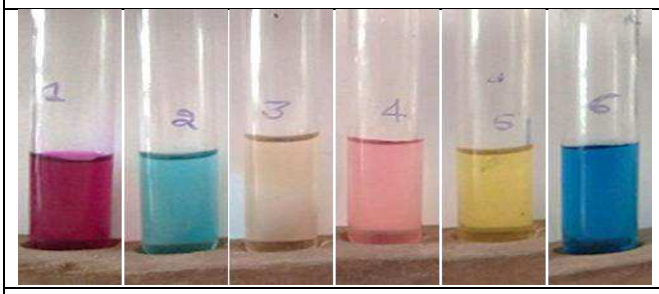	Filter numbers	Optical Density	
	61	0.66	
	49	0.89	
	49	0.56	
	49	0.88	
	49	0.97	
	43	0.86	
Dyes samples with Cobalt - nanoferrites			
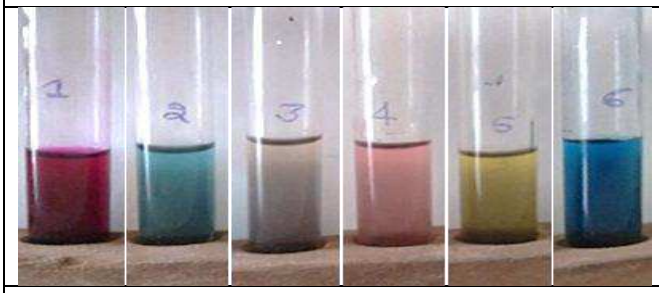	Filter numbers	Optical Density	%
	61	0.57	13.6
	49	0.56	37.0
	49	0.29	48.2
	49	0.58	34.0
	49	0.55	43.2
	43	0.30	65.1
Dyes samples with Zinc - nanoferrites			
	Filter numbers	Optical Density	%
	61	0.51	22.7
	49	0.17	80.8
	49	0.20	64.2
	49	0.32	63.6
	49	0.42	56.7
	43	0.14	83.7

Table 5. Optical Density values of before and after adsorption

% of adsorption of dyes	
Synthesised nanoparticles	% of adsorption
1. Cobalt ferrite nanoparticle	40.1
2. Zinc ferrite nanoparticle	61.9

Table 6. Percentage of adsorption

The mechanism of color change by nano ferrites can be predicted. For example, in phenol red, negatively charged ion denoted as HPS−, the proton from the ketone group of nano ferrites is lost, resulting in the yellow. And at the same time towards higher pH (pKa = 7.7), resulting in the red ion denoted as PS_2−,as the phenol's hydroxy group loses its proton.

Conclusions:

Single-phase cobalt ferrite nanoparticles and Zinc ferrite nanoparticles are synthesized by the chemical wet method. The observed transmittance bands in the range 400–600 cm^{-1} in FTIR spectra approve the establishment of spinel ferrites. SEM images reveal the formation of fine particles within the nanometric range. Nano ferrite of cobalt was synthesized with a particle size of around 50 nm. Sensing studies showed that the sample displays variation in resistance when gases are passed over the surface, and the change in resistance is highest for acetone. Nano ferrite of zinc was synthesized with the particle size of around 90 nm. Sensing studies showed that the sample displays variation in resistance when gases are passed over the surface and the gases sensed in decreasing order of the value of change in resistance obtained are methanol, acetone, ethanol, and ammonia, respectively. The motto of this article is to research and development of ferrite structures, cation distributions, and their impact upon the applications of ferrite components in the adsorption also. Sample B4 holds good for wastewater analysis results and follows the Langmuir isotherm forming the single layer adsorption of acetic

acid on it. Further dye adsorption studies reveal that zinc nano ferrites hold good results of dye adsorption.

Acknowledgements:

The authors acknowledge to the **KLE Society Belagavi,** and **KLE Technological University** (formerly known as B. V. Bhoomaraddi College of Engineering & Technology), for supporting research. This research work is partially supported by B.V. Bhoomaraddi College of Engineering and Technology under "***Capacity Building Projects***" grant reference 2014-15 serial number 14.

References:

[1] C. N. R. Rao, *J. Mater. Chem.* 2004, *14*, DOI 10.1039/b400318g.

[2] C. N. R. Rao, *Nat. Nanotechnol.* 2014, *9*, 564.

[3] S. Ayyappan, G. Diaz De Delgado, A. K. Cheetham, G. Férey, C. N. R. Rao, *J. Chem. Soc. - Dalton Trans.* 1999, 2905–2907.

[4] C. N. R. Rao, *J. Mater. Chem.* 1999, *9*, 1–4.

[5] C. N. R. Rao, J. Gopalakrishnan, *Acc. Chem. Res.* 1987, *20*, 228–235.

[6] G. Cadafalch Gazquez, S. Lei, A. George, H. Gullapalli, B. A. Boukamp, P. M. Ajayan, J. E. Ten Elshof, *ACS Appl. Mater. Interfaces* 2016, *8*, 13466–13471.

[7] U. Mogera, N. Kurra, D. Radhakrishnan, C. Narayana, G. U. Kulkarni, *Carbon* 2014, *78*, 384–391.

[8] S. V. Ganachari, R. Bhat, R. Deshpande, V. A, *Recent Res. Sci. Technol.* 2012.

[9] S. V. Ganachari, L. Hublikar, J. S. Yaradoddi, S. S. Math, *Metal Oxide Nanomaterials for Environmental Applications*, Springer International Publishing, 2019.

[10] V. G. Harris, *IEEE Trans. Magn.* 2012, *48*, 1075–1104.

[11] V. V. Boldyrev, *Solid State Ion.* 1993, *63–65*, 537–543.

[12] R. T. Olsson, G. Salazar-Alvarez, M. S. Hedenqvist, U. W. Gedde, F. Lindberg, S. J. Savage, *Chem. Mater.* 2005, *17*, 5109–5118.

[13] E. Manova, B. Kunev, D. Paneva, I. Mitov, L. Petrov, C. Estournès, C. D'Orléan, J.-L. Rehspringer, M. Kurmoo, *Chem. Mater.* 2004, *16*, 5689–5696.

[14] E. H. Walker, M. L. Breen, A. W. Apblett, *Chem. Mater.* 1998, *10*, 1265–1269.

[15] A. Venkataraman, M. C. Patel, *Thermochim. Acta* 1994, *242*, 249–251.

[16] N. N. Mallikarjuna, B. Govindaraj, A. Lagashetty, A. Venkataraman, *J. Therm. Anal. Calorim.* 2003, *71*, 915–925.

[17] J. N. Behera, C. N. R. Rao, *Inorg. Chem.* 2006, *45*, 9475–9479.

[18] R. Valdez, A. Olivas, D. B. Grotjahn, E. Barrios, N. Arjona, R. Antaño, M. T. Oropeza-Guzman, *Appl. Surf. Sci.* 2017, *426*, 980–986.

[19] I. C. Nlebedim, Y. Melikhov, D. C. Jiles, *J. Appl. Phys.* 2014, *115*, 043903.

[20] S. Gyergyek, D. Makovec, M. Drofenik, *J. Colloid Interface Sci.* 2011, *354*, 498–505.

[21] B. D. Beake, G. A. Bell, S. R. Goodes, N. J. Pickford, J. F. Smith, *Surf. Eng.* 2010, *26*, 37–49.

[22] C. Zhou, A. Zhang, T. Chang, Y. Chen, Y. Zhang, F. Tian, W. Zuo, Y. Ren, X. Song, S. Yang, *Materials* 2019, *12*, 1685.

[23] S. Angappane, N. S. John, G. U. Kulkarni, *J. Nanosci. Nanotechnol.* 2006, *6*, 101–104.

[24] N. Kurra, R. G. Reifenberger, G. U. Kulkarni, *ACS Appl. Mater. Interfaces* 2014, *6*, 6147–6163.

[25] "Improvement of the Magnetic Properties of Mn-Ni-Zn Ferrite by the Non-magnetic Al3+-Ion Substitution," DOI 10.3923/jas.2005.162.168can be found under https://scialert.net/abstract/?doi=jas.2005.162.168, n.d.

[26] N. S. S. Murthy, M. G. Natera, S. I. Youssef, R. J. Begum, C. M. Srivastava, *Phys. Rev.* 1969, *181*, 969–977.

[27] G. Zhang, B. Evans, *Adv. Mater. Phys. Chem.* 2012, *02*, 169–172.

[28] M. Aghazadeh, M. R. Ganjali, M. G. Maragheh, *Int. J. Electrochem. Sci.* 2017, *12*, 5792–5803.

[29] K. Biswas, C. N. R. Rao, *J. Nanosci. Nanotechnol.* 2007, *7*, 1969–1974.

[30] M. M. Eltabey, W. R. Agami, H. T. Mohsen, *J. Adv. Res.* 2014, *5*, 601–605.

[31] Q. Chen, K. Su, M. Zhang, Q. Ma, *J. Non-Cryst. Solids* 2019, *509*, 10–22.

[32] P. Ganguly, C. N. R. Rao, *J. Solid State Chem.* 1984, *53*, 193–216.

[33] G. Vilardi, T. Mpouras, D. Dermatas, N. Verdone, A. Polydera, L. Di Palma, *Chemosphere* 2018, *201*, 716–729.

[34] M. R. Awual, *Chem. Eng. J.* 2017, *307*, 85–94.

[35] S. V. Ganachari, V. K. Joshi, R. Bhat, R. Deshpande, B. Salimath, N. V. S. Rao, V. A, *Int. J. Sci. Res.* 2012, *1*, 77-79–79.

[36] N. N. Mallikarjuna, A. Venkataraman, *Indian J. Eng. Mater. Sci.* 2003, *10*, 50–58.

[37] S. V. Bhat, A. Rastogi, N. Kumar, R. Nagarajan, C. N. R. Rao, *Phys. C Supercond. Its Appl.* 1994, *219*, 87–92.

[38] A. Dąbrowski, *Adv. Colloid Interface Sci.* 2001, *93*, 135–224.

[39] F. R. Bagsican, A. Winchester, S. Ghosh, X. Zhang, L. Ma, M. Wang, H. Murakami, S. Talapatra, R. Vajtai, P. M. Ajayan, et al., *Sci. Rep.* 2017, *7*, DOI 10.1038/s41598-017-01883-1.

[40] P. M. Prithviraj Swamy, S. Basavaraja, A. Lagashetty, N. V. Srinivas Rao, R. Nijagunappa, A. Venkataraman, *Bull. Mater. Sci.* 2011, *34*, 1325–1330.

[41] P. M. Prithviraj Swamy, S. Basavaraja, V. Havanoor, N. V. Srinivas Rao, R. Nijagunappa, A. Venkataraman, *Bull. Mater. Sci.* 2011, *34*, 1319–1323.

[42] A. Venkataraman, V. A. Hiremath, S. K. Date, S. D. Kulkarni, *Bull. Mater. Sci.* 2001, *24*, 617–621.

[43] A. Venkataraman, N. V. Sastry, A. Ray, *J. Phys. Chem. Solids* 1992, *53*, 681–685.

[44] "Microstructure and Superparamagnetic Properties of Mg-Ni-Cd Ferrites Nanoparticles," can be found under https://www.hindawi.com/journals/jnm/2014/492832/, n.d.

[45] "The Potential Theory of Adsorption of Gases and Vapors for Adsorbents with Energetically Nonuniform Surfaces. | Chemical Reviews," can be found under https://pubs.acs.org/doi/10.1021/cr60204a006, n.d.

[46] "Physical adsorption isotherms extending from ultrahigh vacuum to vapor pressure | The Journal of Physical Chemistry," can be found under https://pubs.acs.org/doi/abs/10.1021/j100842a045, n.d.

[47] G. Sankar, P. R. Sarode, A. Srinivasan, C. N. R. Rao, S. Vasudevan, J. M. Thomas, *Proc. Indian Acad. Sci. - Chem. Sci.* 1984, *93*, 321–334.

[48] D. Jacques, J. Šimůnek, D. Mallants, M. T. van Genuchten, *Vadose Zone J.* 2008, *7*, 698–711.

[49] G. Liu, X. Li, L. C. Campos, *J. Water Supply Res. Technol.-Aqua* 2017, *66*, 105–115.

[50] "Removal of Dyes from Wastewater using Adsorption -A Review," can be found under https://www.researchgate.net/publication/255966641_Removal_of_Dyes_from_Wastewater_using_Adsorption_-A_Review, n.d.

[51] S. V. Mohan, J. Karthikeyan, *Environ. Pollut.* 1997, *97*, 183–187.

[52] D. A.O, *IOSR J. Appl. Chem.* 2012, *3*, 38–45.

[53] "Theory for Irreversible and Constant-Pattern Solid Diffusion | Industrial & Engineering Chemistry," can be found under https://pubs.acs.org/doi/abs/10.1021/ie50524a025, n.d.

[54] P. T. Lekkas, "Sorption-desorption isotherms of dyes from aqueous solutions and wastewaters with different sorbent meterials," can be found under https://journal.gnest.org/publication/233, 2013.